Metal–Organic Frameworks

DOI: 10.1002/anie.201007303

Thermal Amorphization of Zeolitic Imidazolate Frameworks**

*Thomas D. Bennett, David A. Keen, Jin-Chong Tan, Emma R. Barney, Andrew L. Goodwin, and Anthony K. Cheetham**

Zeolitic imidazolate frameworks (ZIFs) are a family of metal–organic frameworks (MOFs) that display network topologies analogous to those seen in zeolites whereby the zeolitic building blocks of corner-sharing SiO_4 tetrahedra are replicated by MN_4 tetrahedra (M = metal) linked by imidazolate anions.[1–3] Over 100 distinct ZIF phases adopting 40 network types currently exist.[4] Interest has focused mainly on the tuneable gas sorption and separation properties of these porous materials,[5–7] though their potential for catalytic activity is starting to be explored.[8] The retention of thermal stability derived from their zeolitic structures makes them particularly attractive candidates for practical applications.

Inorganic zeolites are known to undergo pressure- or temperature-induced amorphization.[9–11] Depending on the heating/pressurization rate, the amorphous materials thus formed can retain some aspects of crystalline topology, and consequently possess a lower configurational entropy than true glasses. Polyamorphism (the presence of structurally isomeric amorphous phases differing in density and entropy) has been identified both experimentally and theoretically in these materials.[12] Given the comparison often drawn between between ZIFs and zeolites (ascribed to the common subtended angles of ca. 145° at the metal-bridging species, see Figure 1a), it is not surprising that reports of pressure-induced ZIF phase transitions and amorphization exist,[13–15] albeit at pressures far lower than those of their zeolitic counterparts. Recently, we reported an amorphous ZIF (*a*-ZIF) with a network topology comparable to that of silica glass, formed by thermal amorphization of the crystalline Zn-based ZIF-4 framework. Further heating of the *a*-ZIF yielded the dense ZIF-zni.[16] The mechanical properties of the *a*-ZIF, studied using nanoindentation, were found to be isotropic and intermediate between ZIF-4 and ZIF-zni.

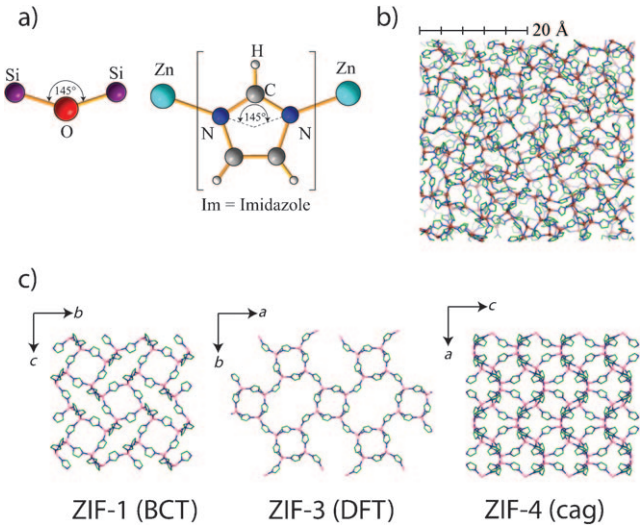

Figure 1. a) The similar Si-O-Si and Zn-Im-Zn linkages in zeolites and ZIFs, respectively. b) A snapshot of the continuous random network (CRN) topology of the *a*-ZIF gained from reverse Monte Carlo (RMC) modeling.[16] c) Representative views of the expanded unit cells of ZIF-1 (left), ZIF-3 (center), and ZIF-4 (right).

Remarkably, the amorphization temperature is comparable to that of purely inorganic zeolites.[17]

Here, we show that *a*-ZIF and crystalline ZIF-zni can also be prepared by heating two structural isomers of ZIF-4 (see Figure 1c). Zn-based ZIF-1 and ZIF-3, possessing the BCT and DFT zeolitic topologies,[18] undergo amorphization and recrystallization to ZIF-zni at similar temperatures to that of ZIF-4. The same process occurs in a cobalt analogue of ZIF-4 (Co-ZIF-4), yielding an amorphous MOF containing a spin-active transition-metal ion. We also show that five ZIFs incorporating substituted imidazolate bridging ions do not undergo thermal amorphization. These frameworks—ZIF-8, -9, -11, -14, and ZIF-βqtz—adopt four different network topologies and possess three different substituted imidazolate species.

Solvothermal reaction of $Zn(NO_3)_2$ and imidazole (Im) under varying conditions yielded single-crystal samples of ZIF-1, ZIF-4, Co-ZIF-4, ZIF-8, ZIF-9, and ZIF-11 of typical size $0.2 \times 0.2 \times 0.1$ mm^3[3,19] whilst a polycrystalline powder sample of ZIF-3 was prepared by a liquid-mixing method.[2] Liquid-assisted grinding was used to synthesize polycrystalline samples of ZIF-14 and ZIF-βqtz.[20]

For ZIF-1, -3, and -4 (Co, Zn) thermogravimetric analysis shows that the structure-directing agent and solvent molecules trapped within the porous cavities of the frameworks are

[*] T. D. Bennett, Dr. J. C. Tan, Prof. A. K. Cheetham
Department of Materials Science and Metallurgy
University of Cambridge, Cambridge CB2 3QZ (UK)
Fax: (+44) 1223-334-567
E-mail: akc30@cam.ac.uk
Prof. D. A. Keen, Dr. E. R. Barney
ISIS Facility, Rutherford Appleton Laboratory
Harwell Oxford, Didcot OX11 0QX (UK)
Dr. A. L. Goodwin
Department of Chemistry, University of Oxford
Oxford OX1 3QR (UK)

[**] We thank T. Abraham, P. Beldon, and Dr. T. Friscic (University of Cambridge) for contributions, and the EPSRC and the ERC for funding to T.D.B., J.C.T., A.L.G., and A.K.C.

Supporting information for this article is available on the WWW under http://dx.doi.org/10.1002/anie.201007303.

lost upon heating to over 200 °C (Supporting Information, SI-1), giving solvent-free isomers of pure $M(Im)_2$ composition. The structural integrity of the frameworks after respective solvent loss was confirmed by powder X-ray diffraction (PXRD). Framework degradation above 450 °C is indicated for all ZIFs studied here, except in ZIF-14, where it occurs at a slightly lower temperature.

Variable-temperature PXRD data from ZIF-1, -3, and Co-ZIF-4 show that on heating amorphization starts at 280 °C, all Bragg reflections disappearing by 300 °C and different Bragg peaks emerging at 370 °C in all three cases (Figure 2). The

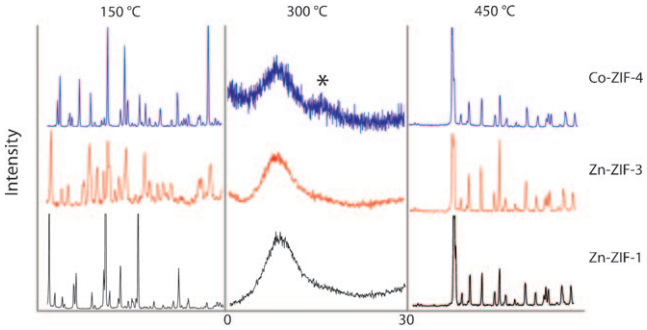

Figure 2. Uncorrected variable-temperature X-ray diffraction patterns for crystalline Zn-ZIF-1, Zn-ZIF-3, and Co-ZIF-4 (left), amorphous phases (center), and recrystallized ZIF-zni phase (right). The reduced quality of the X-ray diffraction pattern for *a*-Co-ZIF-4 relative to the other *a*-ZIF patterns is due to sample fluorescence; the secondary feature (marked with an asterisk) arises from a different background signal when the diffractometer was reconfigured to reduce fluorescence.

transition is irreversible, the resultant amorphous materials (here termed *a*-ZIF-1, *a*-ZIF-3, and *a*-Co-ZIF-4) being recoverable to ambient temperature. Continued heating to above 400 °C resulted in the formation of the dense ZIF-zni phase in all cases. This phase was also recoverable to room temperature and is known to be the most thermodynamically stable of the family.[21]

The amorphization transition was confirmed by differential scanning calorimetry (DSC). Endothermic features indicate desolvation of the framework at 180 °C (ZIF-1 and ZIF-3) and 220 °C (ZIF-4), as well as amorphization at around 310 °C (SI-2). These transition temperatures are broadly consistent with those gained from powder X-ray measurements (considering the different heating rates used in the two experiments). The expected exothermic features belonging to the transition from *a*-ZIF to ZIF-zni were not observed, possibly due to them being smeared out over a large temperature range.

In order to enable comparison with our previous work on *a*-ZIF-4, and indeed other ZIF-related materials,[22] nanoindentation was used to study the mechanical properties of monoliths of *a*-ZIF-1 and *a*-Co-ZIF-4, along with the ZIF-zni microcrystalline phase produced from *a*-ZIF-1 through further heating (Figure 3). The polycrystalline (powder) nature of ZIF-3 prevented the use of nanoindentation in this instance. In the case of Co-ZIF-4, the elastic moduli (E) and hardness (H) properties of the parent phase along the

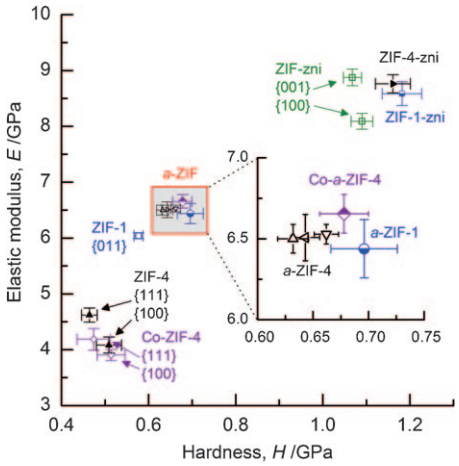

Figure 3. Elastic moduli and hardnesses of the crystalline and amorphous phases of Zn-ZIF-1, Zn-ZIF-4, and Co-ZIF-4 determined by nanoindentation experiments. All parent phases and single crystals of ZIF-zni were indented along known crystallographic orientations readily accessible for a given crystal habit. Because of lower framework density (Table 1), the corresponding facets of the Co-analogue of ZIF-4 exhibit lower stiffnesses. The Zn-ZIF-4 and ZIF-zni data were obtained from Ref. [16] and the three data points of *a*-ZIF-4 (inset) correspond to three orthogonal directions of the monolith. The recrystallized dense phases, that is, ZIF-4-zni and ZIF-1-zni, are microcrystalline.

low-index faces were also measured and found to be anisotropic. The E and H values of the *a*-ZIFs were found to lie between those of the parent phases (i.e. ZIF-1 and Co-ZIF-4, respectively) and ZIF-zni. The similarity of the current amorphous phases to previously reported *a*-ZIF-4 is highlighted by a comparison of their elastic moduli and hardnesses (Figure 3 inset). The elastic moduli obtained for *a*-ZIF-1 and *a*-Co-ZIF-4 lie in the range of 6.3–6.6 GPa, which are within experimental error of those for *a*-ZIF-4 ($E \approx 6.5$ GPa), a striking result when we consider our previous findings that each ZIF has a distinctive E value.[23] The scatter observed in the hardness values is an artefact attributed to surface material pile-up resulting from plastic deformation.[24]

The densities of the *a*-ZIFs, along with those of their parent solvent-containing crystalline phases, were obtained using helium pycnometry (Table 1) and from the unit cells

Table 1: Pycnometric density measurements for the crystalline ZIFs (with solvent) and the amorphous ZIFs (solvent free), together with densities based on lattice parameters determined from PXRD and using the published crystal structures. All densities in $g\,cm^{-3}$.

	Crystalline ZIF (pycnometry)	Crystalline ZIF (PXRD)	Solvent-Free Crystalline ZIF (PXRD)[b]	Amorphous ZIF (pycnometry)
ZIF-1	1.4828(6)	1.4558(10)	1.4524(18)	1.575(4)
ZIF-3	1.1763(20)	0.8832(34)[a]	0.8710(41)[a]	1.572(4)
ZIF-4	1.4616(5)	1.4298(15)	1.4202(21)	1.576(4)
Co-ZIF-4	1.4465(6)	1.3932(16)	1.3917(20)	1.562(6)
ZIF-zni	1.6027(3)	N/A	1.547(68)	N/A

[a] The published structure models the pore-occupying species as a number of water molecule as the exact nature could not be identified. [b] ZIFs were evacuated by heating to 200 °C for 1 h under N_2 and PXRD measurements taken upon cooling to room temperature.

determined by PXRD, in combination with the published crystal structures.[3,19,25] Substantial differences in the parent crystalline phases (due to the inherent structural density and the nature of the pore-occupying solvent) are reflected in the densities. The pycnometric densities of the *a*-Zn-ZIFs compare extremely well with one another and reasonably well with that of *a*-Co-ZIF-4, as expected given the different chemical composition. Indeed, the number density ratio, Zn-ZIF-4:Co-ZIF-4, is very similar whether comparing amorphous, solvated or de-solvated crystalline phases.

Further evidence for the existence of a single amorphous phase was found using total scattering measurements. Total scattering data were collected at room temperature using Ag X-ray radiation ($\lambda = 0.561$ Å) from amorphous samples obtained from the four different crystalline phases. The X-ray total scattering structure factors, $S(Q)$, of the four amorphous ZIFs are compared in Figure 4a with the corresponding pair distribution functions (PDFs) shown in Figure 4b. A calculated $S(Q)$ based on our CRN model of the *a*-ZIF shown in Figure 1b[16] is also included in the inset of Figure 4a, displaying excellent agreement.

The $S(Q)$ of the four *a*-ZIFs are almost identical, each showing smooth broad features and no sharp Bragg peaks. Similarly, the PDFs from the four *a*-ZIFs are very similar. With the exception of the features at very low *r*, where the low statistics in $S(Q)$ at high Q produce variations among the PDFs, each pattern consists of the same sharp features below the metal–metal distance of ca. 6 Å and similar broad features above. In both the $S(Q)$ functions and PDFs the largest differences are found in the Co-ZIF-4 due to the different scattering factors of Zn and Co.

We demonstrated previously that the short-range ordering (SRO) in ZIFs was identical, regardless of whether a crystalline or amorphous material was under consideration.[16] In the CRN model of silica, the limit of the SRO is generally taken as the inter-silicon distance, inclusive of tetrahedral coordination environment and bridging oxygen ions,[26,27] and so here we define the limit of the SRO in ZIFs as the M–M distance (M = Co, Zn) of around 6 Å. It is clear that all four PDFs (Figure 4b) are virtually identical up to the SRO limit, thus confirming retention of the tetrahedral metal environment, along with the bridging imidazolate ion motif.

We assert also that the medium range order, MRO (order extending beyond the nearest and next nearest neighbor distances) has the same form in each *a*-ZIF based on the excellent consistencies across the PDFs (specifically at distances over 6 Å). By analogy with our previous work on *a*-ZIF-4 and the inability of the crystalline starting models to reproduce the *a*-ZIF MRO, we reason that the *a*-ZIFs studied here must also have been formed from reconstructive transitions of the parent $M(Im)_2$ frameworks. The similarity in the $S(Q)$ functions is also suggestive of a common MRO, the identical positions of the first sharp diffraction peak (FSDP) being of particular importance and being used to define a correlation length of up to 5.7 Å, compared with 5 Å in the case of silica.[28] It has recently been proposed that the full width at half maximum (FWHM) of the FSDP can be used to characterize a "coherence length" subdivision of the MRO,[29] which we approximate in the ZIF to be around 10 Å.

Details of the other ZIFs subjected to thermal treatment are provided in Table 2. The materials were subjected to the same heating sequence as ZIF-1, -3, and -4 (Co, Zn), but showed no sign of any thermally induced transition or amorphization in the variable-temperature X-ray experiments. Decomposition was observed at the temperatures indicated by their respective TGA traces (SI-1). The phenomenon of ZIF thermal amorphization appears to be inhibited by the presence of a substituent on the imidazolate species, independent of network topology or substituent size. We believe that this may be due to an increase in the energy

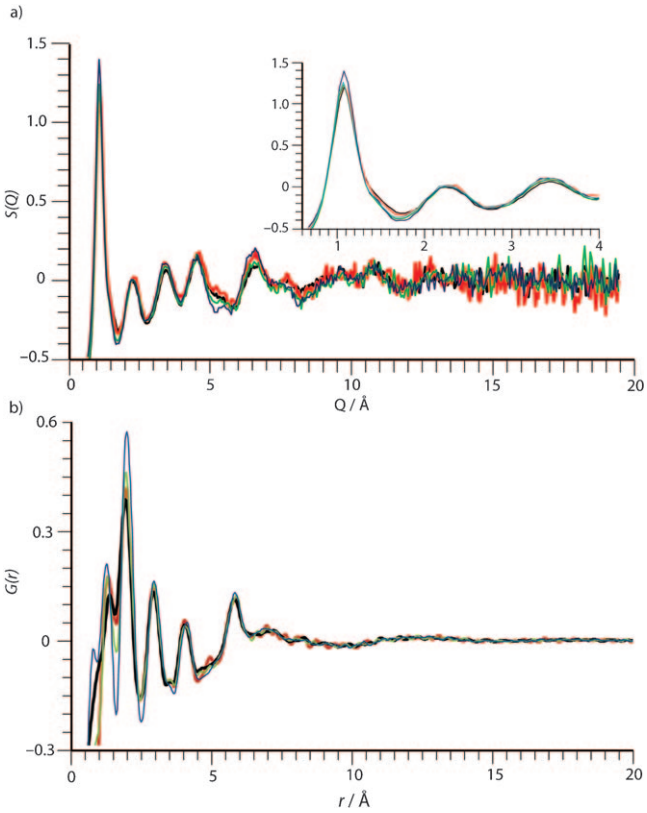

Figure 4. X-ray total scattering data measured for the four amorphous ZIFs. Top: X-ray total scattering function $S(Q)$ for *a*-ZIF-1 (black), *a*-ZIF-3 (red), *a*-ZIF-4 (green), Co-*a*-ZIF-4 (blue), Inset: Low-Q region, including the $S(Q)$ calculated from our CRN model[16] (light blue). (Bottom) Pair distribution function $G(r)$ calculated via Fourier transform of $S(Q)$ up to $Q_{max} = 20$ Å^{-1}.

Table 2: Structural and topological information on the five ZIFs, containing substituted imidazolate linkers.

	Formula	Linker	Network Topology
ZIF-8	$Zn(mIm)_2$	2-methylimidazolate	SOD
ZIF-9	$Co(bIm)_2$	benzimidazolate	SOD
ZIF-11	$Zn(bIm)_2$	benzimidazolate	RHO
ZIF-14	$Zn(eIm)_2$	2-ethylimidazolate	ANA
ZIF-βqtz	$Zn(eIm)_2$	2-ethylimidazolate	βqtz

barrier to reconstructive phase transitions, given the bulkier nature of the ligand.

There is no evidence of polyamorphism in the ZIF family in our work, the same *a*-ZIF being formed regardless of which unsubstituted ZIF is thermally treated. Based on our observations, it is reasonable to anticipate that all other ZIFs encompassing an unsubstituted imidazolate as the only bridging species (specifically ZIF-2, ZIF-6, and ZIF-10) will also undergo thermal amorphization; it necessarily following that this subsection of the ZIF class of materials is not as thermally stable as other members of the family. Generalizations regarding the behavior of those mixed-ligand ZIFs containing an unsubstituted linker along with a substituted imidazolate cannot be drawn. This is an important consideration when the suitability of ZIFs for practical applications is considered.

This work reveals exciting new areas for materials development with respect to the synthesis of functional hybrid glasses. Magnetic studies are currently being carried out on the amorphized Co-ZIF-4 material. It is also likely that amorphous materials with interesting optical and luminescent properties might be accessible through the trapping of a lanthanide ion in one of the more porous crystalline frameworks prior to thermal amorphization.

Experimental Section

ZIF-1 and ZIF-4 (Co, Zn) were synthesized by varying the reported synthesis slightly. All other materials were made exactly according to the synthetic procedures in the given references.[2,3,20]

Zn-ZIF-1: A solid mixture of zinc nitrate hexahydrate $Zn(NO_3)_2{\cdot}6H_2O$ (0.36 g, 1.2 mmol) and imidazole (H-Im) (0.6 g, 8.8 mmol) was dissolved in 72 mL dimethylacetamide in a 100 mL jar. After vigorous stirring the jar was capped tightly and heated to 85 °C for 24 h. The jar was removed from the oven, and after manual cooling to room temperature the mother liquor was decanted. Colorless crystals of ZIF-1 were collected, washed with dichloromethane (DCM) (3 mL × 3), and dried in air (yield 0.09 g, 22 % based on zinc nitrate hexahydrate).

Zn-ZIF-4: A solid mixture of zinc nitrate hexahydrate $Zn(NO_3)_2{\cdot}6H_2O$ (0.12 g, 0.46 mmol) and imidazole (H-Im) (0.09 g, 1.3 mmol) was dissolved in 9 mL DMF in a 20 mL vial. After vigorous stirring the vial was capped tightly and heated to 130 °C for 48 h. The vial was removed from the oven, and after manual cooling to room temperature the mother liquor was decanted. Colorless crystals of ZIF-4 were collected, washed with DCM (3 mL × 3), and dried in air (yield 0.023 g, 18 % based on zinc nitrate hexahydrate).

Co-ZIF-4: A solid mixture of cobalt nitrate hexahydrate $Co(NO_3)_2{\cdot}6H_2O$ (0.14 g, 0.46 mmol) and imidazole (H-Im) (0.09 g, 1.3 mmol) was dissolved in 9 mL DMF in a 20 mL vial. After vigorous stirring the vial was capped tightly and heated to 130 °C for 48 h. The vial was removed from the oven, and after manual cooling to room temperature, the mother liquor was decanted. Purple crystals of ZIF-4 were collected , washed with DCM (3 mL × 3), and dried in air (yield 0.025 g, 19 % based on cobalt nitrate hexahydrate).

The pycnometric densities of Zn based ZIF-1, -3, -4, and Co-ZIF-4, along with the amorphous products derived, were measured using a Micromeritics Accupyc 1340 gas pycnometer (1 cm^3 model). The typical mass used was 0.3 g, with the values quoted being the mean and standard deviation from a cycle of 10 measurements.

The nanoindentation experiments and X-ray total scattering experiments were performed according to the procedures previously described in reference [16].

High-temperature X-ray diffraction data (300–500 K) were collected using a Bruker-AXSD8 diffractometer equipped with a Cu tube and a Ge (111) incident-beam monochromator giving Cu $K\alpha_1$ ($\lambda = 1.540598$ Å) radiation. The diffractometer was operated in Bragg–Brentano geometry with the data collected using a gas-filled Våntec linear position-sensitive detector (PSD). A variable-temperature sample environment of 300–700 K was achieved using an Anton Paar HTK 1200 furnace. For the experiments, a flat sample was mounted onto an amorphous silica disk.

The temperature of decomposition of the substituted ZIFs was gained from their respective TGA curves (SI-1),[3] and the five ZIFs were heated in a tube furnace under a N_2 atmosphere to $T_{decomp.} - 20$ °C for 5 h. PXRD data were obtained while cooling to room temperature; these traces are shown in Figure SI-2.

Received: November 20, 2010
Revised: January 13, 2011
Published online: February 25, 2011

Keywords: amorphous materials · metal–organic frameworks · microporous materials · zeolite analogues · zeolitic imidazolate frameworks

[1] Y. Q. Tian, C. X. Cai, X. M. Ren, C. Y. Duan, Y. Xu, S. Gao, X. Z. You, *Chem. Eur. J.* **2003**, *9*, 5673.
[2] Y. Q. Tian, Y. M. Zhao, Z. X. Chen, G. N. Zhang, L. H. Weng, D. Y. Zhao, *Chem. Eur. J.* **2007**, *13*, 4146.
[3] K. S. Park, Z. Ni, A. P. Cote, J. Y. Choi, R. D. Huang, F. J. Uribe-Romo, H. K. Chae, M. O'Keeffe, O. M. Yaghi, *Proc. Natl. Acad. Sci. USA* **2006**, *103*, 10186.
[4] A. Phan, C. J. Doonan, F. J. Uribe-Romo, C. B. Knobler, M. O'Keeffe, O. M. Yaghi, *Acc. Chem. Res.* **2010**, *43*, 58.
[5] R. Banerjee, A. Phan, B. Wang, C. Knobler, H. Furukawa, M. O'Keeffe, O. M. Yaghi, *Science* **2008**, *319*, 939.
[6] K. Li, D. H. Olson, J. Seidel, T. J. Emge, H. Gong, H. Zeng, J. Li, *J. Am. Chem. Soc.* **2009**, *131*, 10368.
[7] H. Wu, W. Zhou, T. Yildirim, *J. Am. Chem. Soc.* **2007**, *129*, 5314.
[8] J. Lee, O. K. Farha, J. Roberts, K. A. Scheidt, S. T. Nguyen, J. T. Hupp, *Chem. Soc. Rev.* **2009**, *38*, 1450.
[9] G. N. Greaves, F. Meneau, A. Sapelkin, L. M. Colyer, I. A. Gwynn, S. Wade, G. Sankar, *Nat. Mater.* **2003**, *2*, 622.
[10] J. Haines, C. Levelut, A. Isambert, P. Hebert, S. Kohara, D. A. Keen, T. Hammouda, D. Andrault, *J. Am. Chem. Soc.* **2009**, *131*, 12333.
[11] M. Colligan, P. M. Forster, A. K. Cheetham, Y. Lee, T. Vogt, J. A. Hriljac, *J. Am. Chem. Soc.* **2004**, *126*, 12015.
[12] G. N. Greaves, F. Meneau, F. Kargl, D. Ward, P. Holliman, F. Albergamo, *J. Phys. Condens. Matter* **2007**, *19*, 415102.
[13] S. A. Moggach, T. D. Bennett, A. K. Cheetham, *Angew. Chem.* **2009**, *121*, 7221; *Angew. Chem. Int. Ed.* **2009**, *48*, 7087.
[14] K. W. Chapman, G. J. Halder, P. J. Chupas, *J. Am. Chem. Soc.* **2009**, *131*, 17546.
[15] E. C. Spencer, R. J. Angel, N. L. Ross, B. E. Hanson, J. A. K. Howard, *J. Am. Chem. Soc.* **2009**, *131*, 4022.
[16] T. D. Bennett, A. L. Goodwin, M. T. Dove, D. A. Keen, M. G. Tucker, E. R. Barney, A. K. Soper, E. G. Bithell, J. C. Tan, A. K. Cheetham, *Phys. Rev. Lett.* **2010**, *104*, 115503.
[17] G. Cruciani, *J. Phys. Chem. Solids* **2006**, *67*, 1973.
[18] M. O'Keeffe, M. A. Peskov, S. J. Ramsden, O. M. Yaghi, *Acc. Chem. Res.* **2008**, *41*, 1782.
[19] Y. Q. Tian, Z. X. Chen, L. H. Weng, H. B. Guo, S. Gao, D. Y. Zhao, *Inorg. Chem.* **2004**, *43*, 4631.
[20] P. J. Beldon, L. Fábián, R. S. Stein, A. Thirumurugan, A. K. Cheetham, T. Friščic, *Angew. Chem.* **2010**, *122*, 9834; *Angew. Chem. Int. Ed.* **2010**, *49*, 9640.

[21] D. W. Lewis, A. R. Ruiz-Salvador, A. Gomez, L. M. Rodriguez-Albelo, F. X. Coudert, B. Slater, A. K. Cheetham, C. Mellot-Draznieks, *CrystEngComm* **2009**, *11*, 2272.
[22] T. D. Bennett, J. C. Tan, S. A. Moggach, R. Galvelis, C. Mellot-Draznieks, B. A. Reisner, A. Thirumurugan, D. R. Allan, A. K. Cheetham, *Chem. Eur. J.* **2010**, *16*, 10684.
[23] J. C. Tan, T. D. Bennett, A. K. Cheetham, *Proc. Natl. Acad. Sci. USA* **2010**, *107*, 9938.
[24] J. C. Tan, C. A. Merrill, J. B. Orton, A. K. Cheetham, *Acta. Mater.* **2009**, *57*, 3481.
[25] F. Seel, R. Lehnert, E. Bill, A. Trautwein, *Z. Naturforsch. B* **1980**, *35*, 631.
[26] W. H. Zachariasen, *J. Am. Chem. Soc.* **1932**, *54*, 3841.
[27] G. N. Greaves, S. Sen, *Adv. Phys.* **2007**, *56*, 1.
[28] T. Uchino, J. D. Harrop, S. N. Taraskin, S. R. Elliott, *Phys. Rev. B* **2005**, *71*, 014202.
[29] G. Lucovsky, J. C. Phillips, *Nanoscale Res. Lett.* **2010**, *5*, 550.

